Advanced Ceramics Progress: Vol. 7, No. 1, (Winter 2021) 35-45

Advanced Ceramics Progress

Research Article

Journal Homepage: www.acerp.ir

Microhardness Optimization of Al–TiC Nanocomposite Produced by Mechanical Milling and Heat Treatment

J. Arasteh [a] *

[a] *Department of Materials Science and Engineering, Shahid Bahonar university of Kerman, Kerman, Kerman, Iran*

ARTICLE INFO

Article History:

Received 31 December 2020
Received in revised form 19 March 2021
Accepted 17 April 2021

Keywords:

Al–4%TiC
X-ray Diffraction
Milling Parameters
Taguchi Method

ABSTRACT

In this study, the Al–TiC nanocomposite was produced by the mechanical milling and sintering process. Also, the optimization of the milling parameters was performed by the Taguchi method. The X-ray diffraction analysis, scanning electron microscopy, and microhardness test were used to analyze the phase characterization, microstructure, and mechanical properties of the Al–4% TiC nanocomposite. At first, the milling speed, milling time, and ball to powder weight ratio were considered as the input data, and the microhardness was considered as the output value of the Minitab software. According to the design of the experiment, 27 experiments must be performed, which were reduced to 9 by the Taguchi method. After the milling, the powders were subjected to the cold pressing and subsequent sintering at 450 °C. The microhardness results showed that the Al–4% TiC nanocomposite was formed with a maximum microhardness of 271 HV. Furthermore, a proper model was proposed and the results indicated that there was a good agreement between the experimental and predicted microhardness.

https://doi.org/10.30501/ACP.2021.265197.1052

1. INTRODUCTION

Composite materials have been known as superior materials for more than thirty years. In this regard, the application of composite materials has been continuously growing; therefore, many requirements in the various industries, including the space industry, reactor manufacturing, construction, and transportation, cannot be satisfied by the conventional materials and need to change the properties of the materials extensively [1]. Among the composites, Particle-reinforced metal matrix composites (MMCs) are attractive and well-known materials in which hard and brittle particle reinforcements, usually ceramic, are introduced into a ductile metallic matrix [2]. A further improvement of mechanical properties can be achieved by decreasing the grain size to the nanometer scale [3]. Adding reinforcement particles to the aluminum alloys matrix, produces so-called nanocomposites, which is promising approach in order to enhance mechanical properties of the aluminum alloys [1]. These nanocomposites are considered a group of materials with excellent properties such as high strength to weight ratio, low coefficient of thermal expansion, and good wear resistance [4, 5]. Al-based composites are mostly made by distributing the ceramic particles, including SiC, Al_2O_3, TiB_2, or AlWC in the Al matrix [6-9]. Aluminum has excellent properties such as lightweight and ease of machining [10]. Al–TiC composites are one of the most important Al matrix composites with better mechanical properties than the pure Al. Titanium carbide is the appropriate reinforcement due to the high wear resistance, low thermal expansion coefficient, suitable plasticity, and good wettability to improve the properties of Al-based composites [11].

Al matrix composite production techniques in the solid-state such as mechanical milling and sintering process, have received much attention due to differences in the melting point of Al and ceramic particles [7, 12-14]. One of the most exciting advantages of mechanical milling is producing nanocrystalline structures [15]. The scientific research community highly values

* Corresponding Author Email: javadaraste68@gmail.com (J. Arasteh)

http://www.acerp.ir/article_129319.html

Please cite this article as: Arasteh, J., "Microhardness Optimization of Al–TiC Nanocomposite Produced by Mechanical Milling and Heat Treatment", ***Advanced Ceramics Progress***, Vol. 7, No. 1, (2021), 35-45. https://doi.org/10.30501/ACP.2021.265197.1052

nanocrystalline materials due to their high hardness strength and better physical, mechanical and chemical properties compared to coarse-grained materials [16]. Besides, simple equipment of milling process [17], no requirement to the high temperatures [18], and uniform dispersion of reinforcement phase particles in the matrix [19] were included to benefits from the mechanical milling technique. The studies have shown that the properties of the composites produced by mechanical milling are influenced by the microstructure, crystallite size, and morphology so that, these factors are affected by the milling conditions [20, 21]. For examlpe, Azimi and et al. synthesized Al7075-TiC nanocomposite by MA followed by hot pressing. Microstructure of obtained powders was characterized in different milling time. Furthermore, the influence of fabrication parameters including milling time, hot pressing temperature and pressure was evaluated on the mechanical properties. Improved sintering and mechanical properties was achieved by increasing hot pressing temperature and pressure; while rising temperature over 400 °C resulted in reduced hardness due to severe grain growth during hot pressing. More interestingly, influence of milling time on the mechanical properties is strongly depended on the hot pressing pressure value. Furthermore, tensile strength of ~725 MPa was obtained by consolidation under optimal parameters [22]. In another work, Feijoo and et al. produced a composite with a fine-grained AA6005A matrix and 3 vol% nanoparticles of TiC by hot extrusion and T6 heat treatment of high-pressure gas-atomised and mechanically milled powders. The nanocomposites showed remarkably higher hardness, Young's modulus, yield, and ultimate strengths at room temperature than the extruded profiles of unreinforced milled AA6005A powders obtained through refinement of the Al alloy grain structure and a strong particle–matrix bonding, although with a drop in their ductility [23]. Salem and et al showed that addition of TiC nanostructured powder to the AA2124 alloy nanopowder resulted in increase of 130% in compressive strength compared to that produced for the microscale one. Nanopowder of Al alloys produced by mechanical milling reinforced with 10 wt. % TiC is recommended for products suitable for high wear and erosion resistance applications [24].

Therefore, it is necessary to study the milling parameters and examine the effects of the milling parameters on the final product to achieve the optimal conditions. The purpose of experimental design is to identify the parameters influencing the process and determine their optimal values. Experimental design techniques can determine the variables that have the most effect on the output data. In addition, the input variables can be controlled, and the effect of uncontrollable parameters on the response variable can be minimized. Analysis of the results in the experimental design technique is performed by variance analysis (ANOVA). Taguchi method is one of the essential experimental design techniques based on variance analysis [25]. Taguchi method has advantages such as fewer experiments, less cost and time of testing, the ability to study the interactions, perform experiments in parallel, and predict the optimal response. In general, this method reduces the number of required tests for optimization and increases the results' accuracy.

Multiple pieces of research have been recently conducted on the production of Al-based composites by mechanical milling and sintering methods; however, no research has been conducted on optimizing the milling conditions for the production of Al–TiC composites with maximum microhardness by the Taguchi method. In the present study, the design of the experiment was performed by the Taguchi method, and the milling process was performed according to the conditions obtained from the experimental design. In composite fabrication by the milling process, the ball to powder weight ratio is usually between 10 and 30, milling speed is usually between 200 to 400 rpm, and milling time is usually between 10 to 50 hours. In this regard, the values and levels of input data were selected. The parameters of the ball to powder weight ratio (BPR), milling time, and milling speed were considered input data, and the microhardness of the composite was introduced as output data. Furthermore, the most influential parameter was identified and a good proposed model was introduced to predict the microhardness of aluminum-based nanocomposite. The microhardness obtained by the proposed model were compared with the experimental data. Besides, structural characteristics, including phase identification, crystallite size, lattice parameter, internal strain, microstructure, and morphology Al–4% TiC nanocomposite were investigated.

2. MATERIALS AND METHODS

In this study, Al powder (purity of 99.9%, Merck) and TiC powder (purity of 99.9%, Merck) were used as raw materials to produce Al–4% TiC composite. It should be noted that the composition of the Al-4% TiC nanocomposite is expressed by weight percentage. The mechanical milling process was performed in a high energy planetary ball mill. The Al and TiC powders were milled within a hardened steel vial along with hardened steel balls of 10 mm in diameter under a high-purity argon atmosphere. Stearic acid in the amount of 2 wt. % was chosen as a process control agent to avoid cold welding and agglomeration of powder particles. The milling experiments were stopped after each 30 min of working for 15 min to prevent an excessive temperature in the vial. It should be noted MA process was performed at room temperature and dry medium. Usage of cup and balls with the same chemical composition of precursor was the most proposing approach for reducing the

contamination of milling components. Unfortunately, due to the variety of selected systems in MA, it is impossible to make cups and balls from all of the above compounds. An alternative to reduce the impurities was to mill the powder mixture within the range of the studied composition before the start of the main tests. Accordingly, before the data collection step the mixture of each test was milled for 5 h to minimize the variation the chemical composition. The effects of different milling parameters, including the BPR, rotation speed, and milling time on the microhardness of Al–TiC nanocomposite, were studied. In composite fabrication by the milling process, the ball to powder weight ratio is usually between 10 and 30 (The ball to powder weight ratio shows the ratio of the balls' weight to the powders), milling speed is usually between 200 to 400 rpm, and milling time is usually between 10 to 50 hours. In this regard, the values and levels of input data were selected [26-31]. The BPR levels were selected 10, 20, and 30, and the rotation speed of 200, 300, and 400 rpm, and the milling time of 10, 30, and 50 h were considered input data. Before the data collection step, the mixture of each test was milled for 5 hours to minimize the variation of the chemical composition [16]. According to the previous research on the composite fabrication by the milling process, the ball to powder weight ratio is usually between 10 to 30, milling speed between 200 to 400, and milling time for composite preparation is usually between 10 to 50 hours. The levels of parameters have also been selected based on previous works. In this research, three factors with three levels indicated 27 experiments are required to be done according to full factorial design. Taguchi technique was used to design the experiment, which reduced the number of experiments and optimized the milling parameters. According to the experimental design based on the Taguchi technique, nine experiments can be replaced with 27 experiments (Table 1). Moreover, the statistical analysis of variance (ANOVA) was used to determine the effect of the input parameters. The levels of the input data which were chosen for the experiment are shown in Table 1. Finally, the empirical results were compared with the theoretical results obtained from the experimental design.

X-ray diffraction analysis (XRD) was used to investigate the structural changes, phase identification, and determination of the crystallite size, internal strain, and lattice parameter during the MA process. The XRD was performed using an X-ray diffractometer (Cu-Kα radiation and wavelength = 0.154 nm). In this study, the Rietveld method was used to calculate the crystallite size, internal strain, and lattice parameter. In this method, the refining process is performed on the X-ray scattering pattern and continues until the errors are reduced. In other words, the best fit is obtained [32]. It should be noted that the Rietveld analysis was performed using MAUD software [33]. The morphology and shape of the milled powders were studied by scanning electron microscope (SEM, cam scan mv2300). Particle size analyzer (Zetasizer, ZEN3600) was used to determine the powders' particle size. Also, the particle size values were reported as an interval. For microhardness measurement, the milled powders were compressed into a cylindrical shape with a dimension of 1 cm in diameter and a thickness of 0.5 cm. It should be noted that the powder particles were compressed at room temperature and a pressure of 12 tons. The heat treatment was then carried out on the pressed specimens up to 450 °C for 30 min under the argon gas atmosphere. Then, the samples were pressed again at 400 °C after sintering. The surfaces of the specimens were first polished, and the Vickers microhardness test was performed based on the ASTM E 348-89 standard by the microhardness tester (Strues Duramin 20). microhardness measurement was performed with a load of 97.8 mN for 5 seconds. The reported microhardness is an average of 5 times the microhardness of each sample. Also, the Archimedes method was used to measure the density of the samples according to the ASTM, C-373 standard [34].

TABLE 1. The Experiment number proposed by Taguchi method

Experiment number	Ball to powder weight ratio	Rotation speed (rpm)	Milling time (h)
1	10	10	200
2	10	30	300
3	10	50	400
4	20	10	300
5	20	30	400
6	20	50	200
7	30	10	400
8	30	30	200
9	30	50	300

3. RESULTS AND DISCUSSION

Fig. 1 shows the XRD patterns of Al–TiC composite powders at different milling conditions. As is evident, Al–4% TiC composite samples include Al and TiC peaks. It was observed that the peak width was increased; however, the peak intensity was decreased due to the milling process, indicating a decrease in the crystallite size and enhancement of the lattice strain in the crystal structure [35]. The powder particles are severely deformed due to the impact of balls during milling [36]. Hence, the work hardening occurred on the powder

particles. On the other hand, after the milling process, the dislocations were regularly arranged, which caused to form the sub-boundaries in the crystal structure. Continuing the milling process and enhancing the dislocation density in the sub-boundaries led to rotating these boundaries and transforming sub-boundaries into the main boundaries [37].

In this research, Bragg's law was used to estimate the Al lattice parameter [38]. The Al lattice parameter at different milling conditions was shown in fig. 2. As can be seen, there is no noticeable change in the Al lattice parameter owing to the milling process and have a constant trend. The lack of displacement of the Al peaks to the left or right indicates that the TiC was not dissolved in the Al lattice, and the TiC particles were distributed in the Al matrix, which led to applying the local strain in the Al lattice and increased the dislocation density.

The changes in the crystallite size and internal strain of Al–4% TiC composite powders at different milling conditions are shown in Fig. 3.

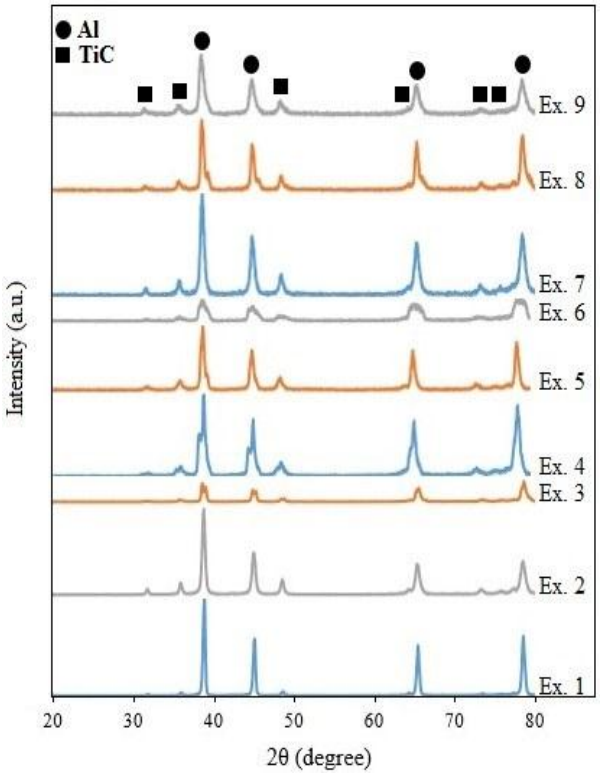

Figure 1. XRD patterns of Al–4% TiC powders milled at different milling conditions

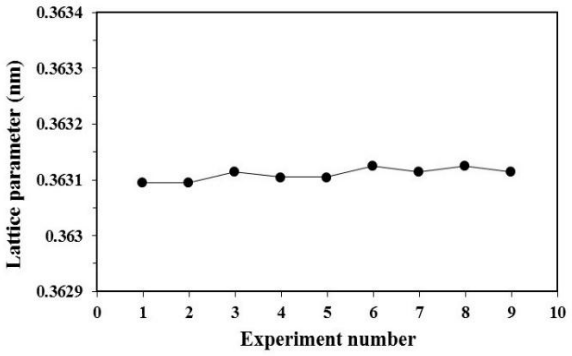

Figure 2. Al lattice parameter changes versus milling condition

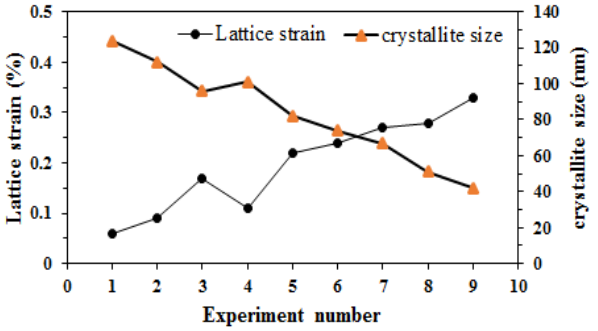

Figure 3. Crystallite size and lattice strain changes of Al at various milling conditions

As shown in this Figure, the crystallite size at each experiment varies according to the milling conditions. Furthermore, at a constant value of the ball to powder ratio, the crystallite size decreased by increasing the milling time and rotation speed. As can be seen, the maximum reduction in the crystallite size is related to experiment number 9 with a ball to powder ratio of 30, a milling time of 50 h, and a rotation speed of 300 rpm. In contrast, the largest crystallite size is associated with experiment number 1 with the lowest milling time. The crystallite size change depended on the plastic deformation and the recovery and recrystallization process [39]. In other words, plastic deformation caused to decrease in the crystallite size; however, the recovery and recrystallization increased the crystallite size. In the present study, the crystallite size of all composite samples decreased after the milling process. The crystallite size range was 42 nm to 124 nm, indicating that the milling process is a proper technique to produce Al–TiC nanocomposite powders. As shown in Fig. 3, the minimum crystallite size of 42 nm is related to experiment number 9 with a ball to powder ratio of 30, a

rotation speed of 300 rpm, and the milling time of 50 h. Furthermore, the maximum crystallite size of 124 nm corresponds to experiment number 1 with the lowest rotation speed of 200 rpm, the milling time of 10 h, and the ball to powder ratio of 10. Since the milling time, the ball to powder ratio, and rotation speed were increased, the lattice defects, internal strain, and the stored energy were increased [40], reducing the crystallite size. The milling significantly increased the strain after the milling process. As can be seen, the strain range of the crystal structure was from 0.06% to 0.33%, which the largest strain was corresponding to experiment number 9.

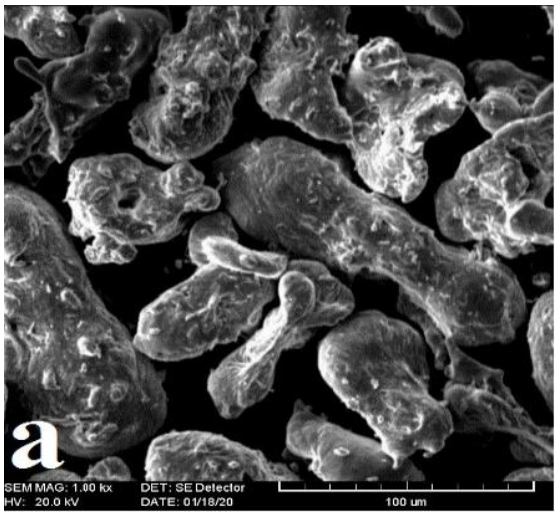

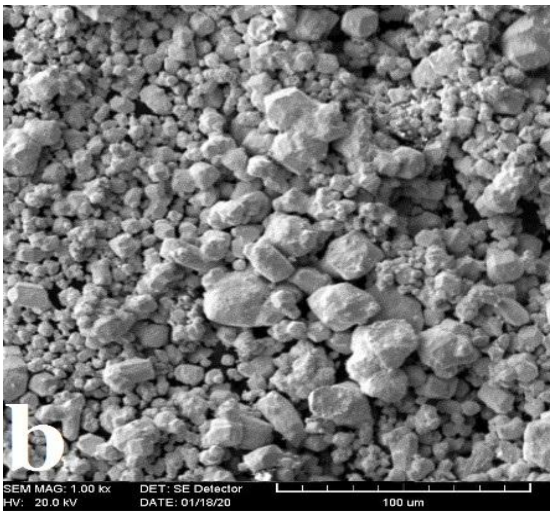

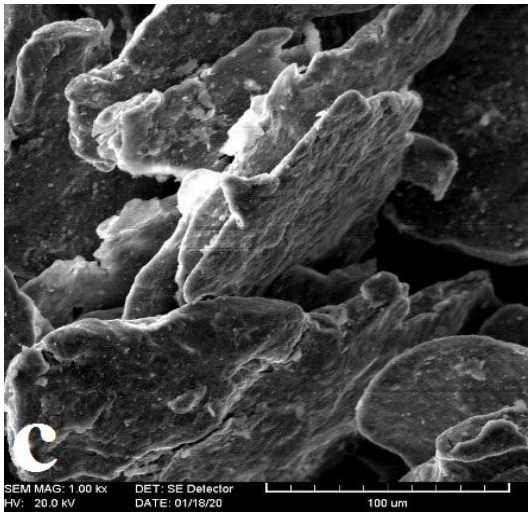

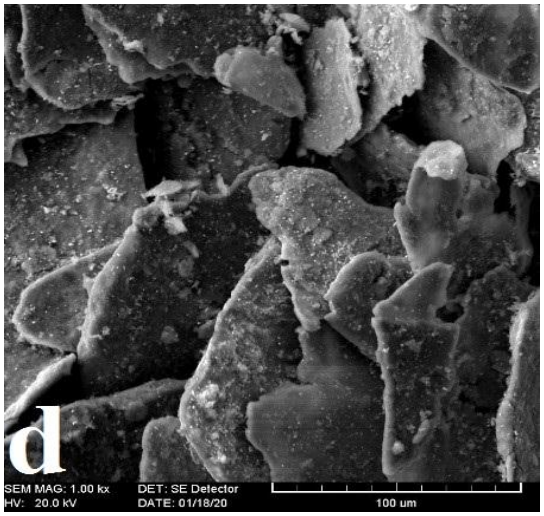

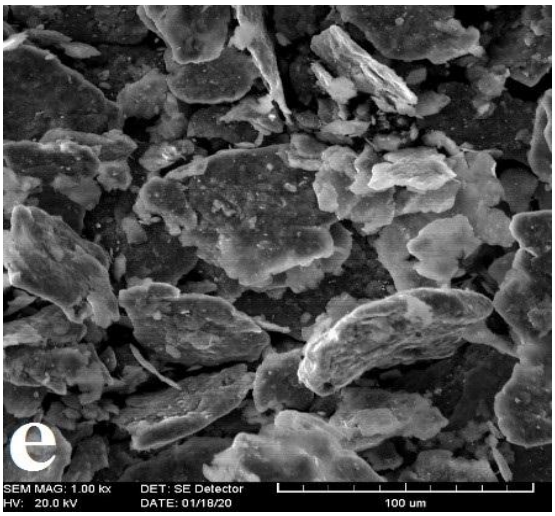

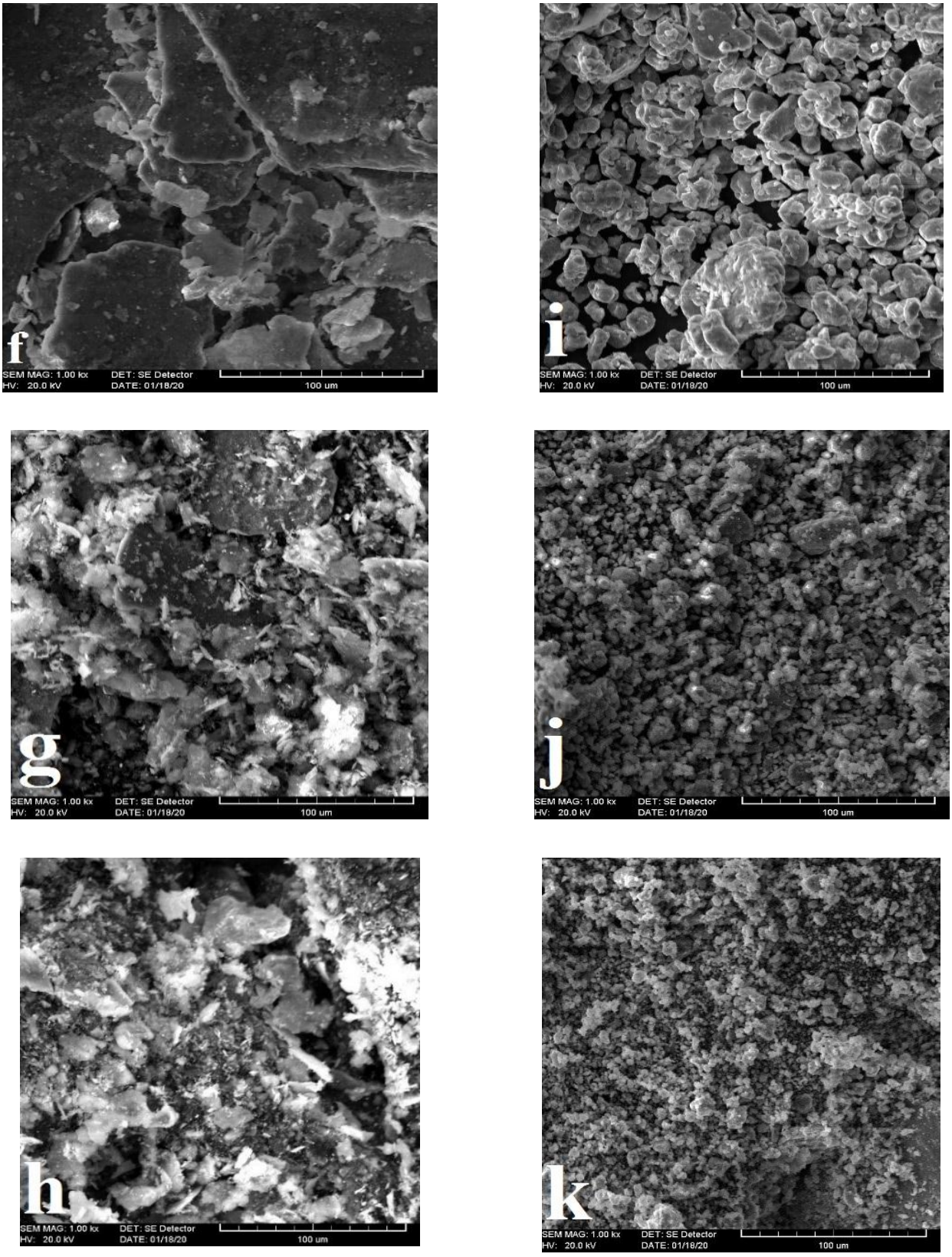

Figure 4. SEM images of Al–4% TiC powders at different milling conditions

Fig. 4 shows the SEM images of the pure Al, TiC, and Al–TiC composite powder particles at different milling conditions. Due to the low value of dislocation density at the beginning of the milling process, the particles were soft and high energy was applied to the powder particles during the MA process. This high energy increased plastic deformation in particles, and powder morphology was shaped as lamellar. In fact, a microforging mechanism caused to overspread the powder particles. Then, cold welding and mechanical joining between the powder particles occurred due to the impacts by the balls. As the milling time increased, dislocation density increased which caused to increase the work hardening of powders. Also, SPD led to form the sessile dislocations and resultantly changed to a mircocrack generation resource. The outcome of these parameters increased the fracture of powder particles and the particle size decreased. In other words, the powder particle fracture phenomenon dominated cold welding and particles size decreased. Finally, the powder particles reached the spherical state and are dispersed more orderly. In fact, the lamella thicknesses decreased due to the continuous deformation, and also, the number of the lamella in one particle increased. Therefore, the diffusion distances decreased. On the other hand, the temperature of powder particles could locally increase due to the energy transfer of the balls. Consequently, the reduction in diffusion distance, the local temperature rise, and the increment of the lattice defects resulted in more diffusion of atoms [37]. As shown in Fig. 4 (a), Al powder particles have an irregular shape and a particle size of 18-130 µm while TiC powders are spherical shape with a particle size of about 1.8-26 µm (Fig. 4 (b)). The powder particles related to experiment number 1 have the largest particle size of about 88-132 µm, thick plate-shaped particles (Fig. 4 (c)). Al powder particles were very soft before milling, and on the other hand, the low energy of milling led to overspread the powder particles. In other words, applied strain due to the milling process caused the powder particles were pressed, and wide particles were cold welding to each other, and finally, the particle size was increased. According to the low energy at experiment number 1 (speed=200, BPR=10, and time=10), the particle size was enhanced compared to the particle size of pure Al. At experiment number 2, the size of the plate-shaped particles was obtained to be about 15-108 µm (Fig. 4 (d)). Also, after experiment number 3, the thickness of the plate-shaped particles was lower than that of experiment number 2, and the particles were irregularly distributed with a size of 3-64 µm (Fig. 4 (e)). The size of plate-shaped particles related to experiment number 4 was found to be 1-100 µm approximately (Fig. 4 (f)).

In experiment number 5, the morphology of powder particles was the combination of plate shape, fine needle, and quasi-spherical with a particle size of 0.5-65 µm (Fig. 4 (g)). In the mechanical milling process, two phenomena of cold welding and fracture occur between powder particles, so that cold welding led to coarsening of the powders while fracture caused to reduction the particle size. The occurrence of these phenomena depended on the properties of powders and the milling. If the powders are brittle, the fracture overcomes the cold welding, and the powders become smaller as the milling time increased, while cold welding is a dominant phenomenon in the soft powders at the beginning of milling. Of course, at longer milling times, the powders get work hardening, leading to powders' fracture and particle size reduction. TiC powder particles were brittle and fractured due to the severe strain during the milling process. Therefore, the reinforcement particles were placed among the Al matrix, which led to work hardening of Al powder particles and reducing the particle size of composite powders. At experiment number 6 (Fig. 4 (h)), the irregular distribution of fine and coarse particles was seen at the particle size range of 0.5-49 µm. As observed in Fig. 4 (i), the particle size was reduced to about 1-39 µm, and the morphology of particles is fine plate-shaped and equiaxed. At experiment numbers 8 and 9, the particles were spherical and regularly distributed with particle sizes about 0.2-59 µm (Fig. 4 (j) and Fig. 4 (k)), indicating that the fracture is a dominant mechanism at this step of milling.

The microhardness values of nanocomposite specimens are shown in Fig. 5. As observed, the microhardness of Al–4% TiC nanocomposite related to experiment number 9 is equal to about 271 HV, which is the maximum microhardness value, and the lowest microhardness is corresponding to experiment number 1 with a value of 221 HV. As the BPR, rotation speed, and milling time were increased, the consolidation behavior of nanocomposite specimens noticeably improved, leading to increased microhardness. It should be noted that the main strengthening mechanisms are the work hardening owing to hard TiC particles within the Al matrix. Also, the lack of dislocation motion during plastic deformation and crystallite refinement can significantly increase the microhardness. It should be noted that the microhardness is affected by the parameters of the ball to powder ratio, milling speed, and milling time and the microhardness does not depend only on the milling speed. Therefore, it can be concluded that the change in microhardness was dependent on the three parameters includes the ball to powder ratio, milling time, and milling speed. The density of the nanocomposites was close to about 94%-98% of the theoretical density. Then, the porosity of the samples was determined by density of sintered sample and theoretical density. The result showed that the porosity of the samples was in the range of 0.02%-0.06%. It should be noted that the theoretical density was determined by the mixtures law.

Fig. 6 shows the results of the microhardness value obtained from the experimental measurement and the data predicted by the Taguchi method. As can be seen,

there is good compatibility between the experimental data and the predicted data. So, it can be concluded that the linear regression model can predict the response parameters. The results of variance analysis related to the microhardness values are presented in Table 2. It should be noted the coefficient of A, B, and C indicate the BPR, the milling time, and the rotation speed, respectively. Also, some statistical data obtained from variance analysis are given in Table 3.

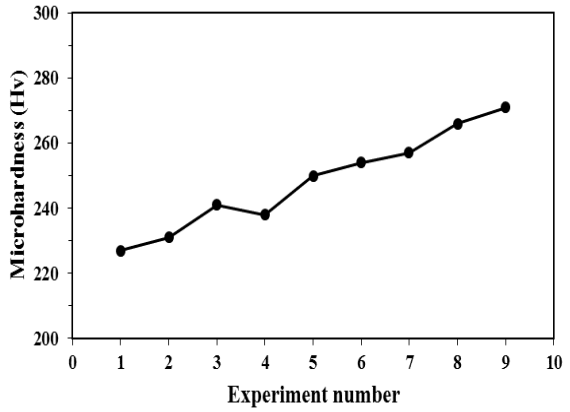

Figure 5. Vickers microhardness values of Al–4% TiC nanocomposites after various milling conditions

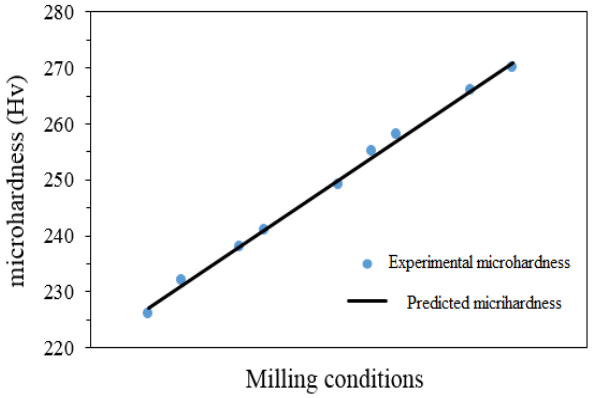

Figure 6. The microhardness values obtained from experimental measurement and Taguchi method

The compatibility of the proposed model and the experimental data is determined by the correlation coefficient (R^2) so that the high value of R^2 (98.7) indicated the good compatibility between the experimental data and the predicted data. The relationship between the process response and the variables number of K in the experiment design is as follows:

$$Y = b_0 \sum_{i=1}^{k} b_i x_i + \varepsilon \quad (1)$$

TABLE 2. The values of Sum of square, Degree of free, Mean square, F-value, and P-value calculated by variance analysis for validation of the proposed model

Source	Sum of square	Degree of free	Mean square	F-value	P-value
Model	1904	3	615	105.4	0.01
A	2242.7	2	1123.6	28.8	0.003
B	448.2	1	472.6	148.5	0.019
C	0.3	1	0.3	99.4	0.03
Error	21	5	5		
Total	1886	8			

TABLE 3. The values of R-parameters estimated by variance analysis

Pred. R-Squared	Adj. R-Squared	R-Squared
95.7%	97.8%	98.7%

Where Y is the process response, b_i is the model parameters, and ε is the error value. The model coefficients are calculated by the Minitab software. The values of model coefficients indicated the effect of the variable on the process response. According to the model coefficients, the ball to powder ratio has the most significant effect on the microhardness value. The effect of milling parameters on the microhardness of Al–4% TiC nanocomposites are shown in Fig. 7. As can be seen, this diagram illustrates the levels of input parameters that have created the maximum and minimum values of microhardness.

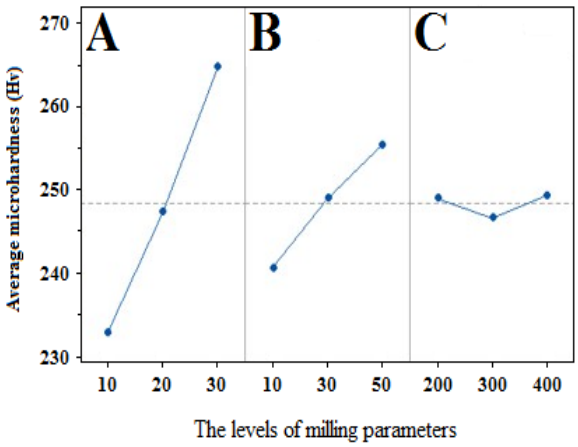

Figure 7. The effect plot of the milling parameters on the microhardness of Al–4% TiC composites

As previously discussed, nine experiments were designed to investigate the effect of milling parameters on the mechanical properties of the Al–4% TiC composites. The P-value in the variance analysis is the smallest level of confidence that leads to the rejection or acceptance of the proposed model. In this research, the P-value was less than 0.05 (95% confidence level), indicating that the proposed model was meaningful and can predict the microhardness values of Al–4% TiC composites. Adj-R^2 (97.8) indicated that 3% of the response changes could not be described with the model. Also, Pred-R^2 indicated a 95% probability of predicting new observations, which had good compatibility with Adj-R^2. The degree of compatibility between the experimental results and prediction results is shown in Fig. 6. As can be seen, there is good compatibility among the prediction data and experimental values. The value of error indicates the deviation of the predicted microhardness from the experimental microhardness. According to the results of this study, it is observed that the predicted and experimental microhardness are consistent. The value of model coefficients indicated the effect degree of the variables on the response. A positive sign of the coefficient indicated a positive effect, and a negative sign indicated an upside-down effect. Based on the coefficients, the proposed model based on the intended variables is as follows:

$$\text{Hardness} = 199.34 + 1.574\,A + 0.332\,B + 0.0015\,C \quad (2)$$

It is observed that the parameters of the ball to powder ratio (A), milling time (B), and milling speed (C) have a positive effect on the hardness. In other words, all three main variables of milling have a meaningful effect on the response.

The diagram of the effect of milling parameters on the microhardness of composites is shown in fig. 7. As can be seen, the highest microhardness of the composites is obtained in the ball to powder ratio of 30, milling time of 50 h, and a milling speed of 400 rpm. Based on these results, it can be expected that the obtained model can predict the microhardness of the composites at other milling conditions with high accuracy, and also experimental design can reduce the time and cost of Al–4% TiC nanocomposite production. The microhardness may be increased by increasing the ball to powder ratio, milling speed, and milling time. However, based on the present conditions, the microhardness was determined, and the result was optimized.

4. CONCLUSION

In this study, Al–4% TiC nanocomposite powders were produced by the mechanical milling process. Furthermore, sintering treatment at the temperature of 450 °C was used for the consolidation of the powder mixtures. Subsequently, based on the experimental design, various conditions of the milling process, including the BPR of 10:1, 20:1, and 30:1, speeds of 200, 300, and 400 rpm, and milling time of 10, 30, and 50 h were considered the input data to finding the maximum microhardness. According to the experimental design, nine experiments were designed by the Taguchi method at certain milling parameters. The results showed that the mechanical milling led to form the Al–4% TiC nanocomposite with a maximum microhardness of about 271 HV. Furthermore, there was good compatibility between the experimental microhardness values and the predicted results by the proposed model by Minitab software. According to the predicted model, the highest microhardness was obtained in the BPR of 30: 1, the milling time of 50 h, and the speed of 400 rpm. In addition, SEM observation indicated that the morphology, particle size, and distribution of powder particles could significantly affect the mechanical properties of the Al–4% TiC nanocomposite so that the maximum microhardness occurred at experiment number 9, which at this condition, the particles were spherical shape and regularly distributed with particle size about 0.2-59 µm. Also, it can be concluded that the properties of the composites were changed because the test conditions of the milling process are different. In general, the mechanical properties of the composite are due to the change in powder morphology, particle size, lattice strain, and crystallite size.

ACKNOWLEDGEMENTS

The author would like to acknowledge the Department of Materials Science and Engineering, Shahid Bahonar university of Kerman for their contribution to this study.

REFERENCES

1. Taghian Dehaghani, M., Ahmadian, M., “Fracture Mechanism of CoCrMo Porous Nanocomposite Prepared by Powder Metallurgy Route”, ***International Journal of Engineering***, Vol. 31, No. 1, (2018), 19-24. https://doi.org/10.5829/ije.2018.31.01a.03
2. Ameri Ekhtiarabadi, T., Zandrahimi, M., Ebrahimifar, H., “The Impact of Current Density of Electroplating on Microstructure and Mechanical Properties of Ni-ZrO_2-TiO_2 Composite Coating”, ***Advanced Ceramics Progress***, Vol. 6, No. 1, (2020), 22-29. https://doi.org/10.30501/acp.2020.105929
3. Nahvi, S. M., “Effect of Carbide Particle Size on the Microstructure, Mechanical properties, and Wear Behavior of HVOF-sprayed WC-17% Co Coatings”, ***Advanced Ceramics Progress***, Vol. 6, No. 3, (2020), 1-14. https://doi.org/10.30501/acp.2020.227010.1033
4. Khoshhal, R., “The Effect of Raw Material Ratios on the Fe-TiC/Al_2O_3 Composite Formation Mechanism”, ***Advanced***

Ceramics Progress, Vol. 3, No. 2, (2017), 25-30. https://doi.org/10.30501/acp.2017.90749

5. Mortazavi, A., Razavi, M., Ebadzadeh, T., Sedaghat Ahangari Hossein Zadeh, A., "Effect of Milling Time on the Crystallite Size and Microstructure of Al_2O_3/Mo Nanocomposite", ***Advanced Ceramics Progress***, Vol. 2, No. 3, (2016), 12-16. https://doi.org/10.30501/acp.2016.70025
6. Sasani, N., Houshyar Sadeghian, M., Khadivi, H., Golestanipour, M., "A Novel, Simple and Cost Effective Al A356/Al_2O_3 Nano-composite Manufacturing Route with Uniform Distribution of Nanoparticles", ***International Journal of Engineering***, Vol. 28, No. 9, (2015), 1320-1327. https://doi.org/10.5829/idosi.ije.2015.28.09c.09
7. Kaushik, N., Singhal, S., "Experimental Investigations on Microstructural and Mechanical Behavior of Friction Stir Welded Aluminum Matrix Composite", ***International Journal of Engineering***, Vol. 32, No. 1, (2019), 162-170. https://doi.org/10.5829/ije.2019.32.01a.21
8. Mitra, R., Chiou, W. A., Fine, M. E., Weertman, J. R., "Interfaces in as-extruded XD Al/TiC and Al/TiB_2 metal matrix composites", ***Journal of Materials Research***, Vol. 8, No. 9, (1993), 2380-2392. https://doi.org/10.1557/jmr.1993.2380
9. Arefkhani, M., Razavi, M., Rahimipoor, M. R., Faeghinia, A., "The Effect of Rotation Speed on the Microstructure and Hardness of Synthesized Al-WC Nano-Composite by Centrifugal Casting", ***Advanced Ceramics Progress***, Vol. 2, No. 4, (2016), 1-6. https://doi.org/10.30501/acp.2016.70031
10. Aswad, M. A., Awad, S. H., Kaayem, A. H., "Study on Iraqi Bauxite Ceramic Reinforced Aluminum Metal Matrix Composite Synthesized by Stir Casting", ***International Journal of Engineering***, Vol. 33, No. 7, (2020), 1331-1339. https://doi.org/10.5829/ije.2020.33.07a.20
11. Mitra, R., Fine, M. E., Weertman, J. R., "Chemical reaction strengthening of Al/TiC metal matrix composites by isothermal heat treatment at 913 K", ***Journal of Materials Research***, Vol. 8, No. 9, (1993), 2370-2379. https://doi.org/10.1557/jmr.1993.2370
12. Mahdavi, M., Khayati, G. R., "Artificial Neural Network Based Prediction Hardness of Al2024-Multiwall Carbon Nanotube Composite Prepared by Mechanical Alloying", ***International Journal of Engineering***, Vol. 29, No. 12, (2016), 1726-1733. https://doi.org/10.5829/idosi.ije.2016.29.12c.11
13. Kuldeep, B., Ravikumar, K. P., Pradeep, S., "Effect of Hexagonal Boron Nitrate on Microstructure and Mechanical Behavior of Al7075 Metal Matrix Composite Producing by Stir Casting Technique", ***International Journal of Engineering***, Vol. 32, No. 7, (2019), 1017-1022. https://doi.org/10.5829/ije.2019.32.07a.15
14. Abbasi, N. F., Azari, K. R., Parvini, A. N., "Synthesis of Nanostructure Ti-45Al-5Cr Alloy by Mechanical Alloying and Study the Effect of Cr Addition on Microstructure of TiAl Alloy", ***International Journal of Engineering***, Vol. 24, No. 2, (2011), 123-130. http://www.ije.ir/article_71898_21fccba5f3ee974387c9075597c7cba7.pdf
15. Rahaei, M. B., Yazdani-Rad, R., Kazemzadeh, A., "Synthesis and Characterization of Nanocrystalline Ni_3Al Intermetallic during Mechanical Alloying Process", ***International Journal of Engineering***, Vol. 25, No. 2, (2012), 89-98. https://doi.org/10.5829/idosi.ije.2012.25.02c.01
16. El-Eskandarany, M. S., "***Mechanical Alloying: Nanotechnology: Materials Science and Powder Metallurgy***", 2nd Ed., Elsevier, Oxford, UK, (2015). http://refhub.elsevier.com/S2468-6069(16)30018-1/sref4
17. Akbari, G. H., Taghian Dehghani, M., "Behavior of Cu-Cr Powder Mixtures During Mechanical Alloying", ***International Journal of Engineering***, Vol. 23, No. 1, (2010), 69-76. http://www.ije.ir/article_71834_380c6a8afec5b5dce8b0fb8825ecf6b5.pdf
18. Nikzad, L., Ghofrani, S., Majidian, H., Ebadzadeh, T., "Effect of ball milling on reactive microwave sintering of MgO-TiO_2 System", ***Advanced Ceramics Progress***, Vol. 2, No. 3, (2016), 25-28. https://doi.org/10.30501/acp.2016.70027
19. Akbarpour Arbatan, M. R., Leisi Azar, F., Alipour, S., "Fabrication of Nanostructured Cu matrix Nanocomposites by High Energy Mechanical Milling and Spark Plasma Sintering", ***Advanced Ceramics Progress***, Vol. 1, No. 3, (2015), 39-43. https://doi.org/10.30501/acp.2015.70011
20. Lou, T., Fan, G., Ding, B., Hu, Z., "The synthesis of $NbSi_2$ by mechanical alloying", ***Journal of Materials Research***, Vol. 12, No. 5, (1997), 1172-1175. https://doi.org/10.1557/jmr.1997.0162
21. Golzar Shahri, M., Shafyei, A., Saidi, A., Abtahi, K., "Effect of CaO on the Formation of PSZ and γ-Zirconia Nanoparticles through Ball Milling", ***Advanced Ceramics Progress***, Vol. 1, No. 2, (2015), 40-44. https://doi.org/10.30501/acp.2015.90747
22. Azimi, A., Shokuhfar, A., Nejadseyfi, O., "Mechanically alloyed Al7075–TiC nanocomposite: Powder processing, consolidation and mechanical strength", ***Materials & Design (1980-2015)***, Vol. 66, (2015), 137-141. https://doi.org/10.1016/j.matdes.2014.10.046
23. Feijoo, I., Merino, P., Pena, G., Rey, P. and Cabeza, M., "Microstructure and Mechanical Properties of an Extruded 6005A Al Alloy Composite Reinforced with TiC Nanosized Particles and Strengthened by Precipitation Hardening", ***Metals***, Vol. 10, No.8, (2020), 1050. https://doi.org/10.3390/met10081050
24. Salem, H. G., El-Eskandarany, S., Kandil, A., Abdul Fattah, H., "Bulk Behavior of Ball Milled AA2124 Nanostructured Powders Reinforced with TiC", ***Journal of Nanomaterials***, Vol. 1, (2009), 479185. https://doi.org/10.1155/2009/479185
25. Rezaei, A. R., Mobasherpour, I., Hadavi, M. M., "An Investigation on Milling Method in Reduction of Magnesium Nano-Powder Particles Based on Sustaining Chemical Activity", ***Advanced Ceramics Progress***, Vol. 4, No. 1, (2018), 12-17. https://doi.org/10.30501/acp.2018.90828
26. Pérez-Bustamante, R., Pérez-Bustamante, F., Estrada-Guel, I., Santillán-Rodríguez, C. R., Matutes-Aquino, J. A., Herrera-Ramírez, J. M., Miki-Yoshida, M., Martínez-Sánchez, R., "Characterization of Al2024-CNTs composites produced by mechanical alloying", ***Powder Technology***, Vol. 212, (2011), 390–396. https://doi.org/10.1016/j.powtec.2011.06.007
27. Zuhailawati, H., Mahani, Y., "Effects of milling time on hardness and electrical conductivity of in situ Cu–NbC composite produced by mechanical alloying", ***Journal of Alloys and Compounds***, Vol. 476, No. 1-2, (2009), 142–146. https://doi.org/10.1016/j.jallcom.2008.09.018
28. Barzegar, M., Vishlaghi, A. A., "Investigation on solid solubility and physical properties of Cu–Fe/CNT nano-composite prepared via mechanical alloying route", ***Powder Technology***, Vol. 47, (2014), 37–42. https://doi.org/10.1016/j.powtec.2014.08.010
29. Sorkhe, Y. A., Aghajani, H., Tabrizi, A. T., "Mechanical alloying and sintering of nanostructured TiO_2 reinforced copper composite and its characterization", ***Materials and Design***, Vol. 58, (2014), 168–174. https://doi.org/10.1016/j.matdes.2014.01.040
30. Sahani, P., Mula, S., Roy, P. K., Kang, P. C., Koch, C. C., "Structural investigation of vacuum sintered Cu–Cr and Cu–Cr–4% SiC nanocomposites prepared by mechanical alloying", ***Materials Science and Engineering: A***, Vol. 528, No. 25-26, (2011), 7781– 7789. https://doi.org/10.1016/j.msea.2011.06.086
31. Basariya, M. R., Srivastava, V. C., Mukhopadhyay, N. K., "Microstructural characteristics and mechanical properties of carbon nanotube reinforced aluminum alloy composites produced by ball milling", ***Materials and Design***, Vol. 64, (2014), 542–549. https://doi.org/10.1016/j.matdes.2014.08.019
32. Dekhil, L., Alleg, S., Bououdina, M., Suñol, J. J., Grenèche, J. M., "Phase transformations and magnetic properties of ball-milled Fe-6P-1.7C powders", ***Advanced Powder Technology***, Vol. 26, No. 2, (2015), 519-526. https://doi.org/10.1016/j.apt.2014.12.011

33. Lutterotti, L., Matthies, S., Wenk, H. R., "MAUD: A friendly java program for material analysis using diffraction", ***IUCr: Newsletter of the CPD***, Vol. 21, (1999), 14-15. https://www.iucr.org/__data/assets/pdf_file/0016/21634/cpd21.pdf
34. Kumar, A. A., Patton, M. R., Hennek, J. W., Lee, S. Y. R., Alesio-Spina, G. D., Yang, X., Kanter, J., Shevkoplyas, S. S., Brugnara, C., Whitesides, G. M., "Density-based separation in multiphase systems provides a simple method to identify sickle cell disease", ***Proceedings of the National Academy of Sciences***, Vol. 111, No. 41, (2014), 14864-14869. https://doi.org/10.1073/pnas.1414739111
35. Patankar, S. N., Xiao, S. Q., Lewandowski, J. J., Heuer, A. H., "The mechanism of mechanical alloying of $MoSi_2$", ***Journal of Materials Research***, Vol. 8, No. 6 (1993), 1311-1316. https://doi.org/10.1557/jmr.1993.1311
36. Schoenitz, M., Dreizin, E. L., "Structure and properties of Al-Mg mechanical alloys", ***Journal of Materials Research***, Vol. 18, No. 8, (2003), 1827-1836. https://doi.org/10.1557/jmr.2003.0255
37. Dieter, G. E., Bacon, D. J., "***Mechanical Metallurgy***", Vol. 3, New York: McGraw-Hill, (1986). https://dokumen.tips/documents/mechanical-metallurgy-by-dieterpdf.html
38. Cullity, B. D., Stock, S. R., "***Elements of X-ray Diffraction***", 3rd Eds., Prentice-Hall, New York, (2001). https://www.pearson.com/us/higher-education/program/Cullity-Elements-of-X-Ray-Diffraction-3rd-Edition/PGM113710.html
39. Eckert, J., Holzer, J. C., Krill, C. E., Johnson, W. L., "Structural and thermodynamic properties of nanocrystalline fcc metals prepared by mechanical attrition", ***Journal of Materials Research***, Vol. 7, No. 7, (1992), 1751-1761. https://doi.org/10.1557/jmr.1992.1751
40. Suryanarayana, C., "Mechanical alloying and milling", ***Progress Materials Science***, Vol. 46, No. 1-2, (2001), 1-184. https://doi.org/10.1016/s0079-6425(99)00010-9